Supporting Information

Revealing the mechanism for rapid growth of organic-inorganic halide perovskite crystals

Pabitra K. Nayak[1a], David T. Moore[2a], Bernard Wenger[1], Simantini Nayak[3], Amir A. Haghighirad[1], Adam Fineberg[4], Nakita K. Noel[1], Obadiah G. Reid[2], Garry Rumbles[2], Philipp Kukura[4], Kylie A. Vincent[3], Henry J. Snaith[1]*

[1]Clarendon Laboratory, University of Oxford, Parks Road, Oxford, OX1 3PU, UK

[2]National Renewable Energy Lab, Golden, CO 80401, USA

[3]Department of Chemistry, University of Oxford, Inorganic Chemistry Laboratory, South Parks Road, Oxford, OX1 3QR, UK

[4]Physical and Theoretical Chemistry Laboratory, University of Oxford, South Parks Road, Oxford,OX1 3QZ, UK

[a] Equal contribution

E-mail **henry.snaith@physics.ox.ac.uk**

Materials:

We bought DMSO, DMF, NMP, carboxylic acids, PbI_2, $PbBr_2$, and $PbCl_2$ from Sigma Aldrich, GBL from Alfa Aesar, MAHI and MAHBr from Dyesol, and MAHCl from Merk. We used the chemicals as received without further purification.

Experimental Methods:

Synthesis of γ-hydroxybutyric acid (GHB)

20mL of fresh, neat GBL was added dropwise to 15mL of .02 M NaOH solution while stirring, a precipitate forms immediately. After complete addition the solution was stirred for 30 minutes and the precipitate, NaGHB salt, recovered using a rotovap. The salt was then dissolved in ~15 mL of 1.2 M HCl in water; the precipitate, NaCl, was dried in a rotovap and the liquid recovered. The recovered liquid consisted of GHB, water, and unreacted HCl. The final recovery was done by boiling off the remaining water/HCl at 60 °C for 48 hours. The distillation was taken to be complete when the remaining liquid formed a very viscous liquid and the pH, measured in water, matched the calculated pH of pure GHB.

Preparation of $CH_3NH_3PbBr_3$ crystals in NMP:

We prepared 1 M solution of the bromide salts (MAHBr + $PbBr_2$) in NMP and added 60 µl of FAH per 1 ml of NMP. To grow single crystals of $MAHPbBr_3$, we kept the resulting solution in a closed cap vial and incubated at 80 °C. Under similar conditions, solution without FAH did not yield any crystals.

Preparation of $CH_3NH_3PbBr_3$ crystals in DMSO:

We prepared 1.5 M bromide salt solution in DMSO and added 400 µl of FAH per 1 ml DMSO. We placed the resulting solution in a vial and placed in an oil bath at 105 °C and noticed crystallization within 5 minutes of incubation. A control vial without FAH did not produce any crystals even after several hours of incubation.

Preparation of cm scale $CH_3NH_3PbCl_3$ crystal at 55°C in DMSO:

We prepared 2 M solution of the chloride salts in DMSO and heated at 80 °C with constant stirring for 2 hours to get clear solution and then cooled down to room temperature. We then used 5 mL of the solution and added 200 µl of formic acid to it and filtered the solution using a 0.45 micron filter. We kept the solution in a closed cap vial at 55 °C to produced seed crystals. We then prepared another solution this time 150 µl of formic acid /5 ml of the salt solution. In a 30 ml vial, we put a cleaned Si wafer at the bottom of the vial, poured the solution into the vial and carefully put a seed (~500 µm scale) crystal of $MAHPbCl_3$ on the Si substrate. We then closed the cap of the vial and put that in an oil bath kept at 55 °C. The crystals grew on the Si substrate and we collected the crystal when they reached the desired size. When we wanted bigger size crystals, we added fresh solutions to the vial and allowed the crystals to grow further.

Preparation of cm scale $CH_3NH_3PbBr_3$ crystal at 55 °C in DMF:

We prepared 1 M solution of the bromide salts in 5 ml DMF and then added 150 µl of formic acid to the solution followed by a filtration with 0.45 micron filter. We used a 30 ml vial and put a cleaned Si wafer at the bottom of the vial. We then poured the solution into the vial and carefully put a seed (~500 µm scale) crystal of $MAHPbBr_3$ on the Si substrate. We follow the same procedure for crystal growth that we described for the chloride system. We note

here that the amount of FAH needed to grow the crystals at 55 °C may vary depending on the existing FAH in the DMF as a degradation product.

Preparation of cm scale $CH_3NH_3PbI_3$ crystal at 55 °C

We prepared iodide salts solution at 1.2 M in 5 ml fresh GBL by dissolving the salts at 55 °C with vigorous stirring for at least 30 minutes. The growth of the initial seeds and the subsequent 1 cm crystal was as described above for the chloride crystals except that the FAH volume added was 14.5 vol%. Crystals were grown at 50, 70, and 100 °C by adjusting the molarity to 1.3, 1.0, and 0.8 M respectively and adjusting the volume % of FAH to 16.0, 10.0, and 10.0 vol% respectively.

Absorbance:

We collected the absorption spectra using a Perkin-Elmer Lambda 1050 UV-Vis spectrophotometer in transmission mode.

X-ray single crystal diffraction and analysis:

We collected the single crystal data at 293 K using an Agilent Supernova diffractometer that uses Mo K_α beam with λ = 0.71073 Å and is fitted with an Atlas detector. We did the data integration and cell refinement using CrysAlis Pro Software, analysed the structure by Patterson and Direct methods, and refined using SHELXL 2014 software package.

In situ electrochemical measurements:

For electrochemical measurements, we used a Mettler Toledo SevenEasy™ pH meter in potential mode using an InLab Micro glass probe. We prepared samples in 22mL vials with the probe inserted through a septum cap and measured on a hotplate with constant stirring; we used equivalent vials of solvent only to monitor temperature with a temperature probe. We recorded both temperature and potential in 1s increments.

We measured each sample at room temperature (RT) for a period sufficient to stabilize the system, typically 30-45 minutes. Then we raised the temperature to ~80 °C and left for 30-45 minutes. After that we turned off the heater and allowed the system to cool back to RT.

We calibrated the pH probe before and after each measurement with a three point buffer set. Whenever we saw a difference in the offset >10 mV we cleaned the probe thoroughly, changed the internal electrolyte and repeated the measurement (for reference at 20 °C, in water, the potential change is ~59mV/pH). Prior to the use of a new solvent, we cleaned the probe and changed the electrolyte then calibrated the probe.

For temperature correction we used the following equation

$$E_{measured} = E_0 + 2.3\frac{RT}{F}\log\frac{a(H^+)}{a(H_0{}^+)}$$

where $E_{measured}$ is the recorded potential, E_0 is the temperature corrected potential of the probe, T is the temperature, R and F are the gas and Faraday constant respectively, $a(H^+)$ is the proton activity of the sample and $a(H_0{}^+)$ is the proton activity of the internal probe standard. We experimentally measured the value for E_0 using a buffer of pH7.0 over the temperature range of interest.

For neat, pure solvents, a constant in situ measurement was not possible with the experimental apparatus used due to the lack of any salt or an appreciable concentration of acid in the system. Therefore, the potential change for the pure, neat solvents (black diamonds in Fig. 1b and S3) were taken by recording 3 separate measurements for each temperature of interest; measurements were recorded during 60 s after a 60 s stabilization time and the values for all 3 measurements averaged. In the case of DMF and GBL these measurements were performed during the same experimental session, and using the same solvent, as the samples plotted in the accompanying plots.

<u>In situ ATR- IR spectroscopy:</u>

Instrument details: We used an Agilent FTIR spectrometer with liquid nitrogen cooled Mercury Cadmium Telluride (MCT) detector for in situ IR spectroscopy. For multiple reflections of incident IR light, we used a modified ATR accessory (GladiATR, PIKE Technologies) placed inside the spectrometer.

ATR crystal and IR cell: We used a Si trapezoidal ATR reflection element with a dimension of 5 x 8 x 1 mm^3 and 39˚ angle of incidence at both short edges (Crystal GmbH, Germany).

Before each experiment, the Si crystal was cleaned with isopropanol followed by deionized water. The IR cell was developed in-house for in-situ experiments.[1] The Si crystal was attached to the baseplate of the IR cell with epoxy glue to prevent leakage during solution flow through the cell. A glass vial fitted with a rubber septum, placed in a copper heating block, was used as a solvent reservoir. To circulate the salt solution between the reservoir and the IR cell, we used a peristaltic pump (flow speed: 5 mL min^{-1}) fitted with thermally insulated tubing. The schematic arrangement is shown in Figure S1. To increase the temperature of the solution, we heated the copper block and monitored the temperature of the solution in the cell by insertion of a thermocouple. Spectra were recorded at 5 $^{\circ}C$ intervals. IR data are presented as absorbance spectra with reference spectra collected at a bare Si ATR reflection element. Spectra were collected at a spectral resolution of 4 cm^{-1} and presented as 250 co-added scans.

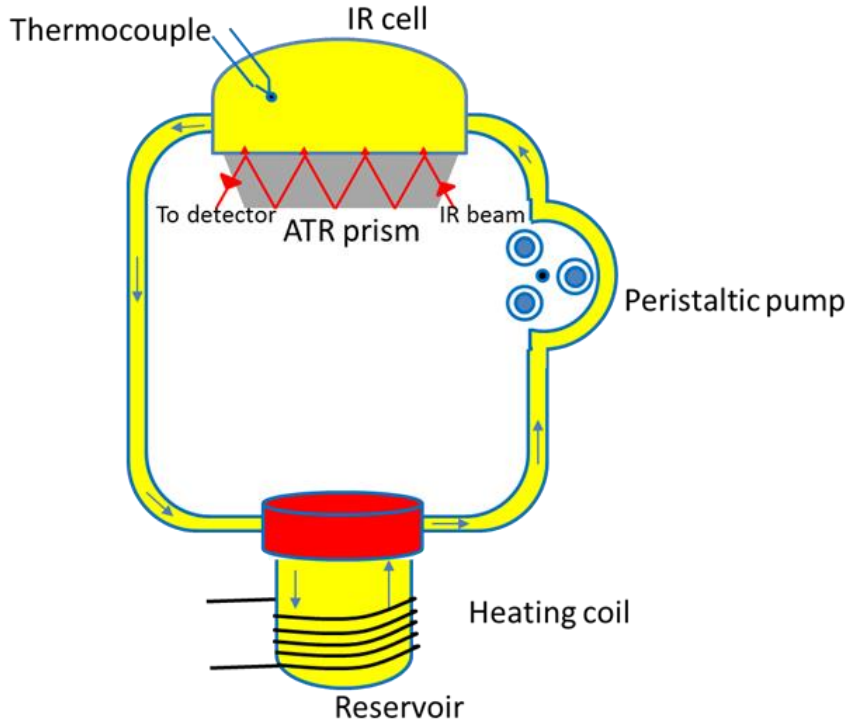

Figure S1: Schematic diagram of in situ IR spectroscopy set up. The circulation of solution between the reservoir and the cell is shown by blue arrows.

<u>Interferometric scattering microscopy (iSCAT):</u>

We used a custom-built iSCAT microscope[2,3] to follow the Colloidal aggregate dynamics and perovskite crystal growth. The microscope setup is as follows. A 635nm diode laser (Lasertack) serves as the light source with P-polarization output. The collimated laser beam pass through two acousto-optic deflectors (AODs, Gooch & Housego), rapidly scanning the beam in two dimensions. A 4f telecentric lens system images the deflection generated by the AODs into the back focal plane of a high numerical aperture microscope objective (Olympus PlanApo, 60x, 1.42 NA). Before entering the objective the beam passes through a polarizing beam splitter (PBS), to allow for separation of the illumination and detection channels, and a quarter waveplate (QWP). A 45-degree mirror couples the illumination light into the objective. The objective collects the light reflected from the glass/sample interface together with the back-scattered light from the sample. After a second pass through the QWP, the light becomes s-polarized, and the PBS reflects scattered and reflected light into the detection channel. A 1m focal length achromatic doublet (Thorlabs) forms an image onto a CMOS camera (Photonfocus), with a magnification of 333x and a nanometre to pixel conversation of 31.8nm/px.

We cleaned the coverglass thoroughly by ultrapure water (Milli-Q) and ethanol. We then incubated the cover glass in a 50:50 mixture of isopropanol and ultrapure water for 15 minutes in a sonicator bath. After a final rinse with ultrapure water, we blow dried the coverslips with nitrogen. We then placed a clean 20µl volume silicone gasket (Grace Bio-Labs) firmly on top of the clean coverglass and then the solution to be imaged within. We used a flexible polyimide foil heater (Thorlabs) wrapped around the microscope objective and temperature controller (Thorlabs) to control the sample heating during imaging.

We captured images at 10Hz. The exposure time for colloidal dissolution and crystal growth were 7ms and 0.01ms, respectively.

Static light scattering (SLS):

A quartz cuvette, placed on a temperature controlled stage with a magnetic stirrer, serves as the container for the salts solutions. A 4.5 mW, 532 nm CW laser (Thorlabs CPS532) acts as the light source which is measured using a Si diode (Thorlabs det36/a) positioned at the right angle to the light beam and in front of one of the walls of the cuvette. An optical

chopper modulates the incident laser beam, and a lock-in amplifier (Stanford Research Systems SR810) acquires the data from the Si diode.

We prepared 1M solution of MAHI + PbI_2 in GBL, 1M solution of MAHBr + $PbBr_2$ in DMF and 2M solution of MAHCl + $PbCl_2$ in DMSO. We stirred the stock solutions with a magnetic stirrer at 50°C for few hours before bringing it to the room temperature. We used 2ml of the solution for scattering experiment.

We raised the temperature at 5°C step size and waited for 2 minutes at each point before collecting the intensity of the scattered light. The rotation speed of the stirrer in the cuvette remained constant during the entire experiment. For MAHCL + $PbCL_2$ in DMSO, we heated the solution up to 70 °C and then brought back to 25°C and measured the scattered light intensity for 2 hours which was stable over the time range. In the MAHBr + $PbBr_2$ in DMF system, after the formation crystals, the solution was brought back to 10°C and kept there for a rapid dissolution of crystals, and then the temperature was raised for additional measurements.

1- (1P) and 2-photon (2P) photoluminescence:

The 1P photoluminescence spectrum was recorded in air using 532 nm excitation and off-axis front face detection geometry in a commercial spectrometer (Horiba Fluorlog) equipped with a nitrogen cooled CCD detector. Various sample angles between 0 and 15 degrees off-normal from the incident beam were tried, verifying that the spectra recorded were not influenced by small variations in the angle of incidence.

2P photoluminescence measurements were carried out in a sealed, nitrogen filled cell with fused quartz windows. Photoexcitation was provided by a Nd:YAG pumped OPO (Spectra Physics Quanta Ray and GWU Premi Scan) with a pulse-width of 5.6 ns, FWHM. Intensity was controlled by a set of neutral density filters downstream of the OPO and measured by a pyroelectric power meter (Coherent USB-10MB-LE). The laser light was focused by a 500 mm focal-length fused quartz lens to a spot size of ~ 0.02 cm^2 (wavelength dependent). The long focal length ensures little change in spot size as the excitation beam passes through the sample, and thus provides a uniform probe of the bulk of the sample without artifacts from a localized focal volume.

Photoluminescence was detected in off-axis front-face geometry. The PL detection system consists of a 50 mm f/0.95 C-mount camera lens (Thorlabs MVL50HS) mounted onto a filter holder (Thorlabs CFH2) with a silicon APD (Thorlabs APD430A) attached to the other side, transducing transient optical signals with DC-400 MHz bandwidth. An 800 ± 10 nm bandpass filter (Thorlabs FB800-10) was used to block excitation light, and pass a reasonable amount of both observed emission bands from the sample. The whole assembly is mounted to a pitch-yaw kinematic stage for easy alignment with the emission spot. The signal from the APD was digitized using a fast oscilloscope (Tektronix DPO7254), and successive pulses were averaged in software to obtain clean transient signals and the associated standard deviation.

Extended Data

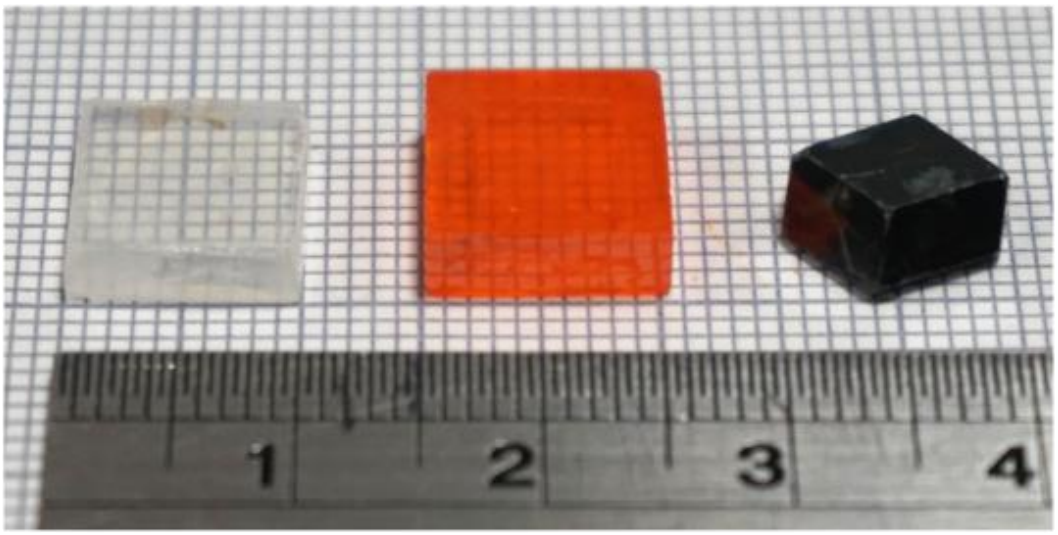

Figure S2: Optical image of cm scale crystals of $MAHPbCl_3$, $MAHPbBr_3$ and $MAHPbI_3$ grown at 55 °C

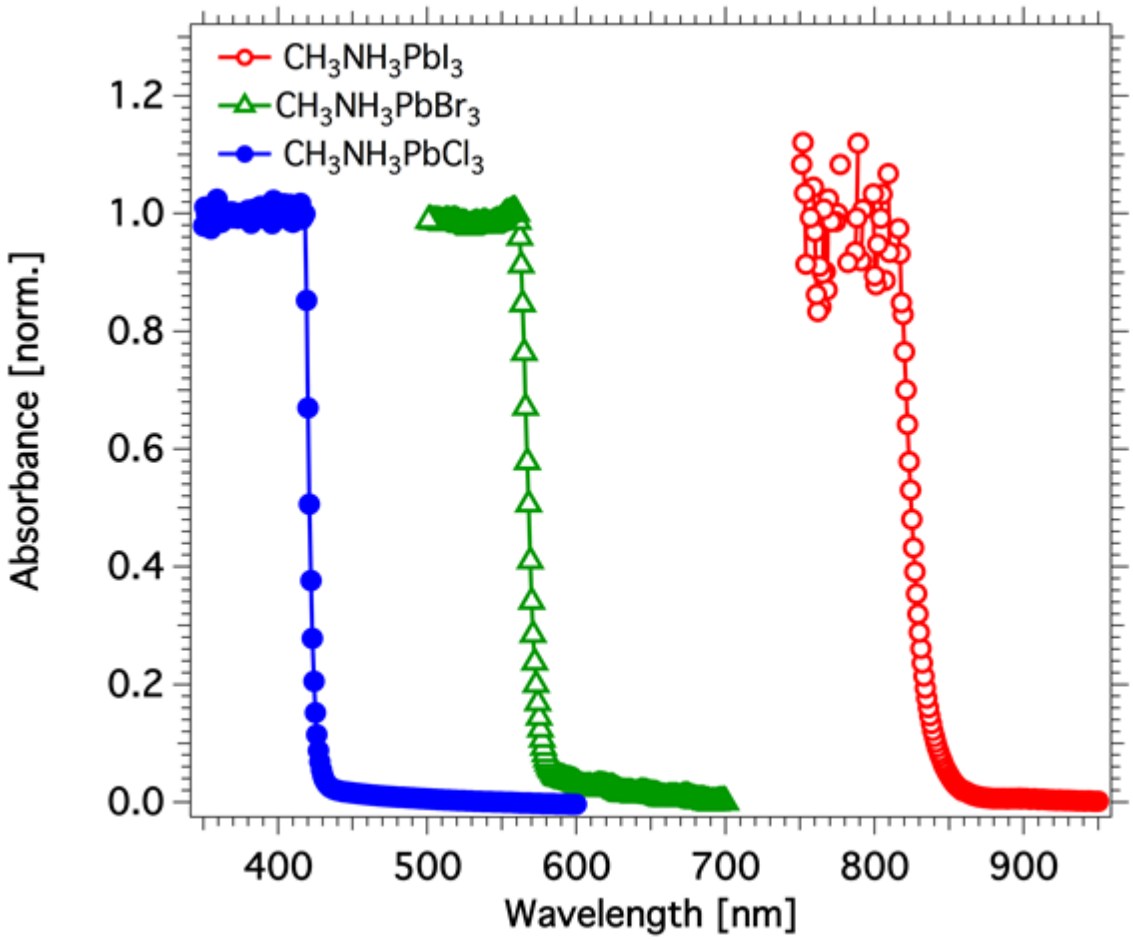

Figure S3: Normalized absorption spectra for $CH_3NH_3PbCl_3$ (blue, filled circles), $CH_3NH_3PbBr_3$ (green, open triangles), and $CH_3NH_3PbI_3$ (red, open circles)

Table S1: Crystallographic data of $CH_3NH_3PbCl_3$,$CH_3NH_3PbBr_3$ and $CH_3NH_3PbI_3$ single crystals at RT.

Compound	$CH_3NH_3PbCl_3$	$CH_3NH_3PbBr_3$	$CH_3NH_3PbI_3$
Growth temperature	328 K	328K	328 K
Measurement temperature	293 K	293 K	293 K
Space group	*Pm-3m*	*Pm-3m*	*I4/m c m*
Unit cell dimensions	a = 5.688 ± 0.005 Å α = β = γ = 90°	a = 5.928755 ± 0.000078 Å α = β = γ = 90°	a = 8.878 ± 0.005 Å c = 12.643 ± 0.005 Å α = β = γ = 90°
Volume	184.03 $Å^3$	208.40 $Å^3$	996.73 $Å^3$
Z	1	1	4
Density (calculated)	3.119 g/cm^3	3.817 g/cm^3	4.131 g/cm^3
Reflections collected	2804	2308	7946
Unique reflections	53	60	261
R(int)	0.1580	0.2554	0.1255
R (sigma)	0.0298	0.0476	0.0278

Goodness-of-fit	0.868	0.518	1.217
Final R indices	0.0383	0.0409	0.0560
Wavelength	0.71073 Å	0.71073 Å	0.71073 Å
Weight scheme for the refinement	Weight = 1 / [$sigma^2(Fo^2)$ + (0.1034 * P)^2 + 0.00 * P] where P = (Max (Fo^2, 0) + 2 * Fc^2) / 3	Weight = 1 / [$sigma^2(Fo^2)$ + (0.1184 * P)^2 + 34.99 * P] where P = (Max (Fo^2, 0) + 2 * Fc^2) / 3	Weight = 1 / [$sigma^2$ (Fo^2) + (0.0681 * P)^2 + 82.13 * P] where P = (Max (Fo^2, 0) + 2 * Fc^2) / 3

In situ pH measurement of GBL and DMF

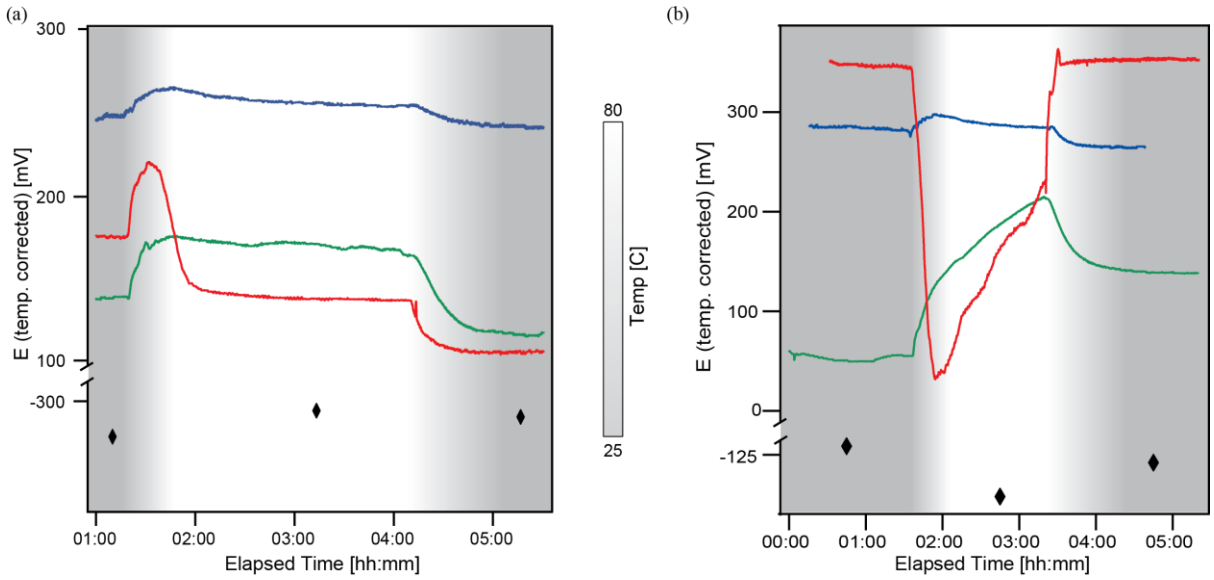

Figure S4: Electrochemical measurements for (a) DMF with bromide salts, and (b) GBL with iodide salts; neat solvent (black diamonds), with 1 M salts (green), with 3 vol% FAH (red), and with 1 M salts and 3 vol% FAH (blue). All potential data has been temperature corrected; temperature is denoted by the background color with the scale bar centered in between the plots.

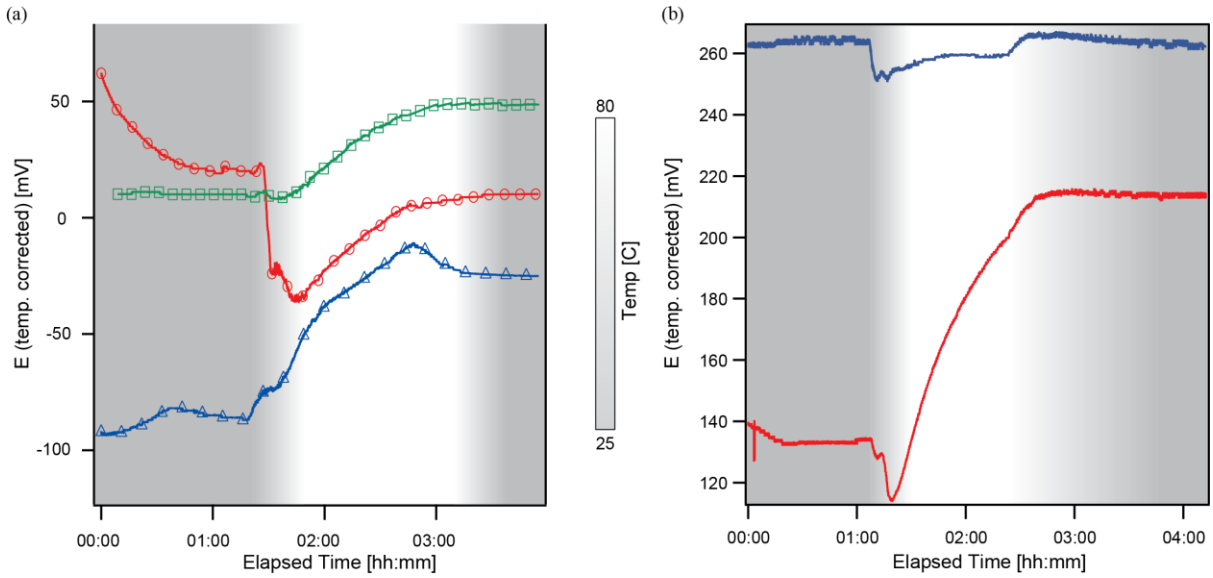

Figure S5: Potential measurements for neat solvents during heating; all potential data has been temperature corrected with the temperature denoted by the background color with the scale bar centered in between the plots. (a) fresh, anhydrous DMF (red circles), the same sample immediately after the first heating cycle (green squares), and 3 month old DMF (blue triangles); (b) fresh, anhydrous GBL (red), and 1 month old GBL stored in ambient, after an initial 24 hours at 60 °C, with the septum cap removed (blue).

Figure S4 shows the erratic behaviour of the solvent with only acid added which is similar to the behaviour of the neat solvents in Fig. S5. For GBL and DMF this is to be expected as they already contain some concentration of carboxylic acid. Therefore, addition of a similar acid only increases or decreases this behaviour (depending on the solvent age) but it is still erratic and not completely reversible. Despite this behaviour with the solvent/acid samples, for the complete system: solvent, acid, and salts; the change in acidity is of similar magnitude and completely reversible for all systems tested.

<u>In situ ATR-IR measurement</u>

We chose the chloride salt system in DMSO as neat DMSO does not produce any carboxylic acid as degradation product, does not show any change in the proton activity upon heating and has no IR absorption peak in the 1800-1450 cm^{-1} region where we expect to see the carbonyl (from carboxylic acid) and N-H (from MA and MAH^+) vibrational modes. Figure S6 shows the ATR-IR absorption spectra of neat DMSO, DMSO containing MAHCl and $PbCl_2$ and DMSO containing FAH. The absorption peaks at 1500 cm^{-1} and 1625 cm^{-1} are due to the symmetric and asymmetric bending modes of N-H in MA and MAH^+, respectively. The intensity of these peaks should reflect the degree of protonation of MA due to the change in

symmetry (Cs for MA and C3v for MAH^+) .[4] For carboxylic acids, absorbance around ~1750-1700 cm^{-1} is due to the carbonyl stretching and its intensity decreases up on deprotonation.[5] Figure S7 shows IR spectrum of MAHCl + $PbCl_2$ in DMSO with different amount of FAH. We see that addition of more FAH causes an increase in the absorbance of the IR modes associated with carbonyl stretching as well as N-H bending.

In figure S8 we show the temperature dependent IR absorbance of 1.5 M MAHCl + $PbCl_2$ in DMSO with 5 vol % FAH at 5 °C intervals from 25 °C to 55 °C. We see a monotonic decrease in absorbance for the carbonyl stretching vibrations (~1700-1750 cm^{-1}) and monotonic increase for the N-H vibrations (at 1500 cm^{-1} and 1620 cm^{-1}) as the temperature rises. We attribute this to the deprotonation of FAH and protonation of MA on heating.

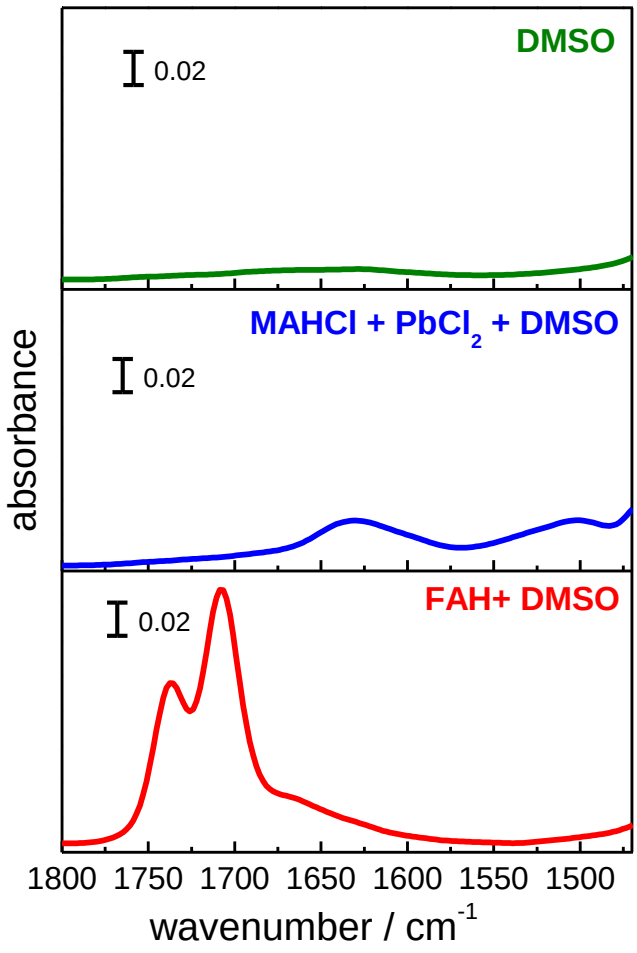

Figure S6: IR spectra of neat DMSO (top), MAHCl + $PbCl_2$ in DMSO (middle) and formic acid in DMSO

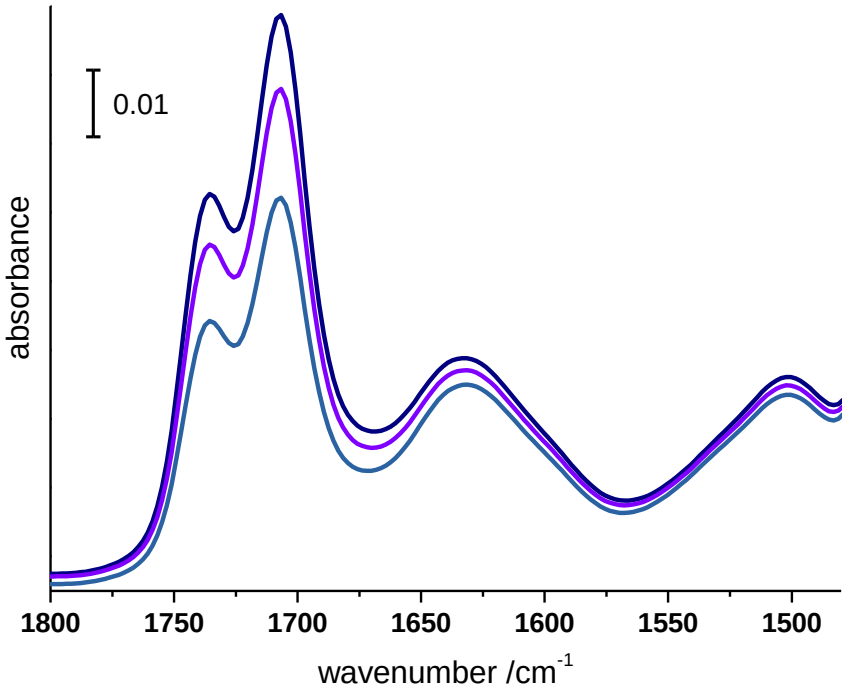

Figure S7: IR spectra of MAHCl + $PbCl_2$ in DMSO with different quantity of formic acid.

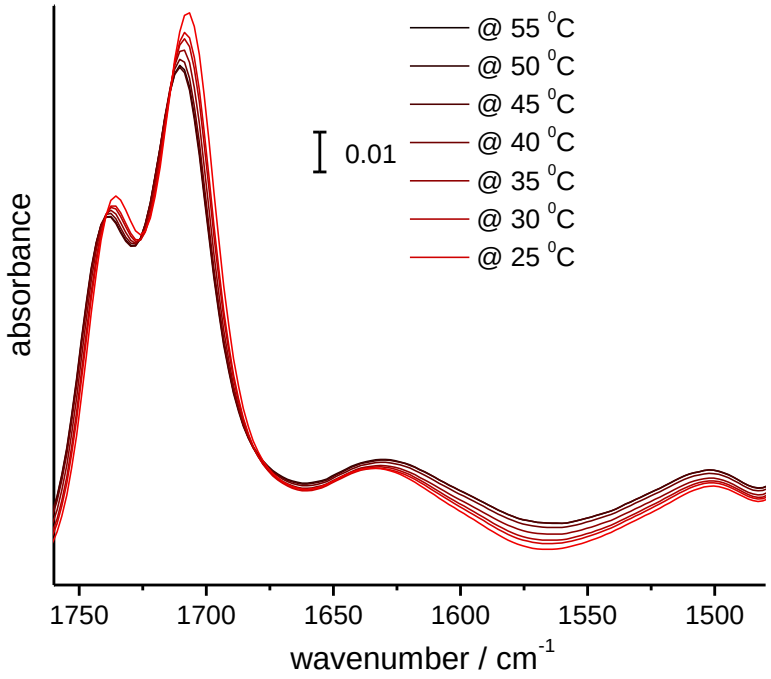

Figure S8: Temperature dependent in situ IR spectra of 1.5 M MAHCl + $PbCl_2$ in DMSO with 5 vol% formic acid.

Test of MA on solvent strength

To understand the effect of MA on the solution strength, we prepare a 1M solution of MABr + $PbBr_2$ in DMF and incubate the solution at 100°C to produce single crystals of $CH_3NH_3PbBr_3$. After 2 hours of incubation, when there is no noticeable further growth of the crystals, we assume that the crystals are in equilibrium with the solution. Then we bubble MA gas through the solution for 5 minutes, while maintaining the crystallisation temperature, and find that the crystals dissolve back into the.

Effect of partial removal of colloids from the solution:

To test the effect of colloids in crystallization, we prepare 1 M solution of bromide salts in DMF and iodide salts in GBL. We stir the iodide salt solution at 70°C for 30 minutes before bringing it to the room temperature. We then centrifuge the solutions at 14800 rpm for 8 minutes. After centrifugation, we collect the supernatant solutions, depleted in colloidal particle concentration. In the Figure S9 (a) and (b) we show the optical images of 1 M solution of MAHI + PbI_2 in GBL, and supernatant solution after centrifugation. We see that the supernatant solution is visibly clearer than the original solution which we attribute to the partial removal of colloidal particles. When we raise the temperature of the solutions, $MAPbI_3$ crystals start to form at ~110 °C in the original solution (Fig. S9c) unlike the supernatant solutions where we do not observe any crystal formation until 150 °C (Fig. S9d). Similarly for the $MAPbBr_3$ system, when we raise the temperature to 85 °C we see the crystal formation in the original solution (Fig S9e) unlike its less colloid containing counterpart where the onset of crystallization is at 120 °C (Fig. S9f). As we show in Fig S9 (g) and (h), the yield of the crystals is less in the supernatant solution compared to the original solution under similar conditions.

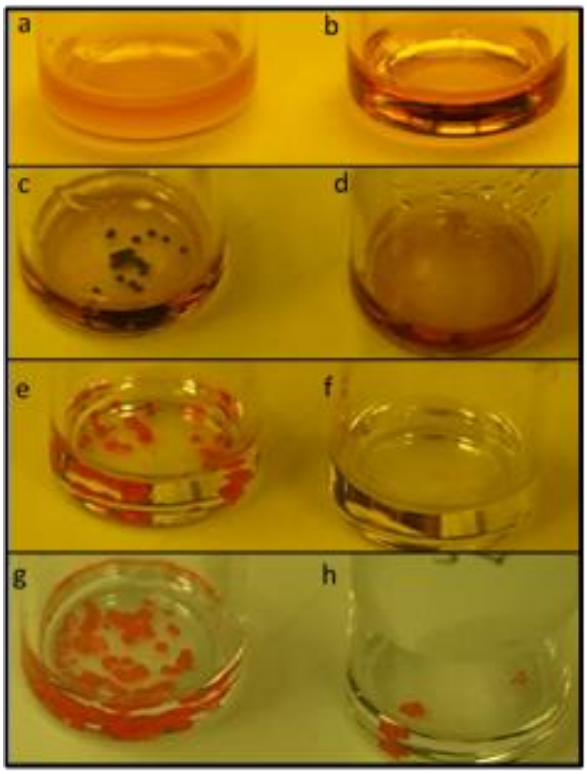

Figure S9: Effect of colloids on crystallization. (a) and (b) show the optical images of 1 M salt solution of MAHI +PbI_2 in GBL and supernatant solution after centrifugation, respectively. (c) and (d) show the images when the original and supernatant solution of the iodide salts are incubated at 110°C, respectively. (e) and (f) show the images for 1M MAHBr +$PbBr_2$ solution in DMF and its supernatant solution incubated at 85°C, respectively. (g) and (h) show when the above-mentioned bromide salt solutions are incubated at 120 °C where a higher yield of crystals happens for the original solution.

SLS and iSCAT Data:

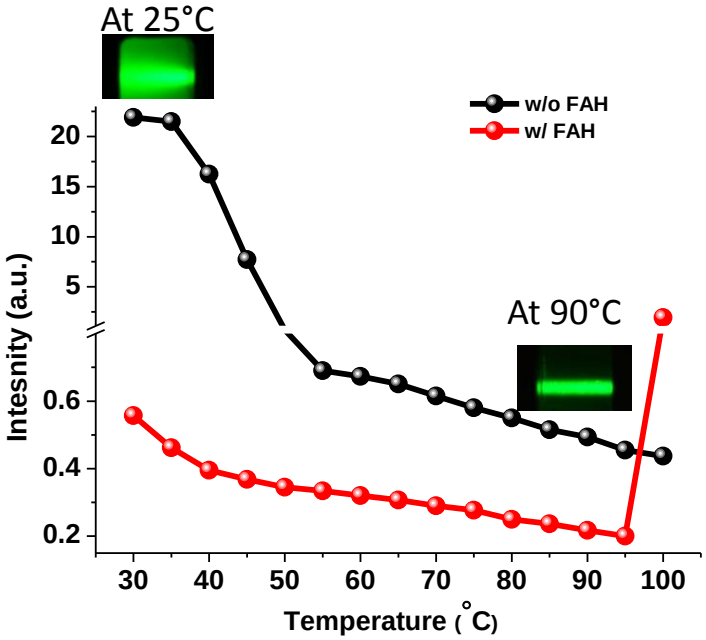

Figure S10: : Effect of added acid and temperature on the scattered light intensity of 1 M MAI + PbI_2 in GBL, Insets show images of laser beam through 1 M MAI + PbI_2 at 25°C and at 90°C.

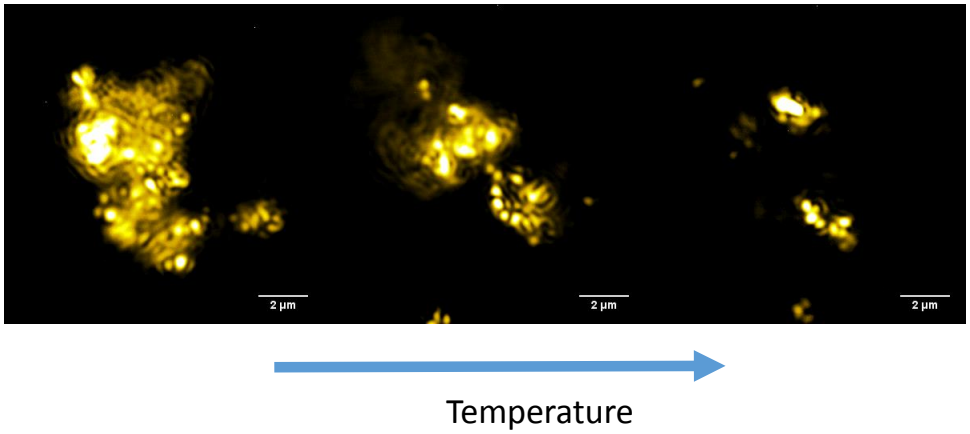

Figure S11 : Sequence of events (a-c) during heating of a 1 M iodide salt solution in GBL (temperature range 25°C to 50°C)

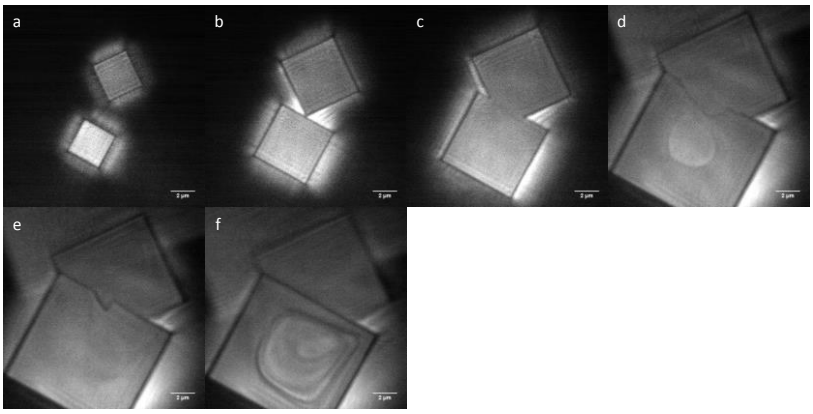

Figure S12: Sequence of events (a-f) showing the growth of $CH_3NH_3Br_3$ crystal formation where the crystals are growing from clear solution rather than from detectable colloids.

Hypothesis Tests

Effect of acid/base strength

We test our proposed mechanism by intentionally disrupting the acid/base equilibria and observing the impact on the crystallisation in a solution of 1 M bromide salts in DMF. When we add a weaker base, aniline (protonated base pKa=3.8 in DMSO), than MA (protonated base pKa=11.0 in DMSO) to the solution we expect no change in the crystallisation behaviour as the MA will be preferentially protonated during heating.[6] When we add a stronger base, 1,1,3,3-Tetramethylguanidine (TMG) (protonated base pKa=13.2 in DMSO), we expect the stronger base to be protonated, in lieu of MA, which should inhibit the

crystallisation. In both test cases the behaviour we observe matches our expectations (See Figure S13).[6]

Finally, we crystallise the iodide system in GBL isothermally at 70 °C by addition of FAH; once the crystals have formed we add a slightly stronger base to the solution (butylamine, protonated base pKa=11.1 in DMSO) and the crystals dissolve; i.e. we crystallise by addition of acid and reverse it by addition of base.[6]

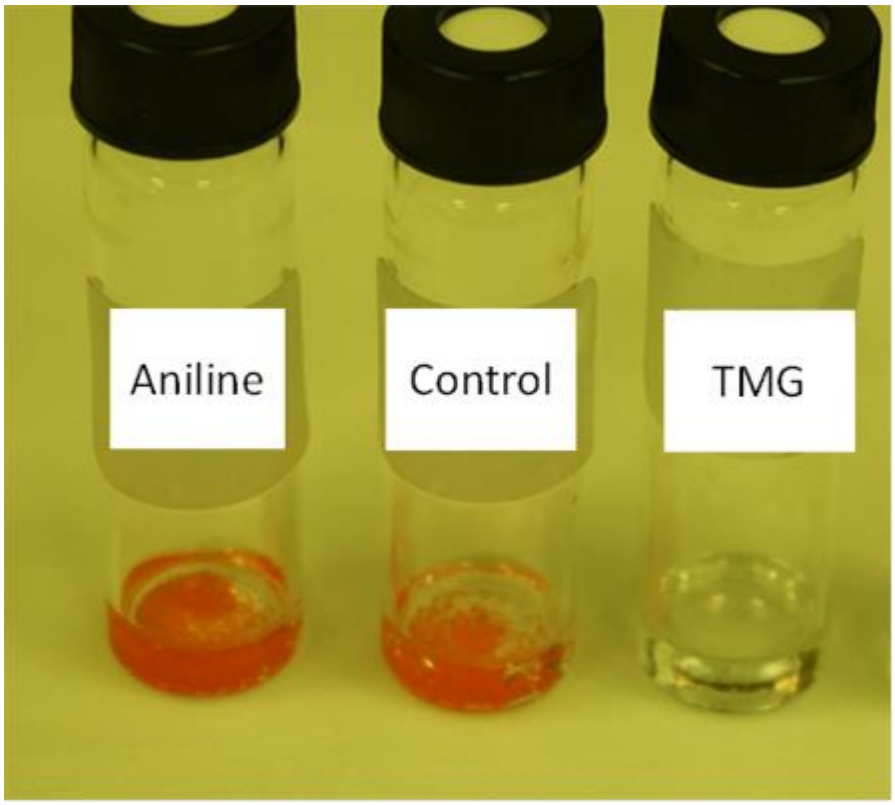

Figure S13: Growth of $CH_3NH_3PbBr_3$ crystals in DMF with weaker / stronger base. A weaker base (Aniline) does not inhibit the crystal formation while a stronger base (TMG) does.

Test of FAH as an anti-solvent:

To find out whether FAH is an anti-solvent for perovskites like chlorobenzene (CB), we added 5 mg of $MAPbI_3$ powder (prepared by crushing single crystals of $MAPbI_3$ in and mortar and pestle) to vials containing 1ml of FAH and CB. We then stirred the solution for 30 minutes. We then measure photoluminescence (PL) of the solutions. While the CB solution showed the PL corresponding to the $MAPbI_3$, the FAH solution did not show the same behaviour. Figure S14 shows the optical image of the vials containing CB and FAH solution

containing $MAPbI_3$ powders. In FAH solution, $MAPbI_3$ powder does not survive in its perovskite form, thus FAH is not a typical antisolvent like CB.

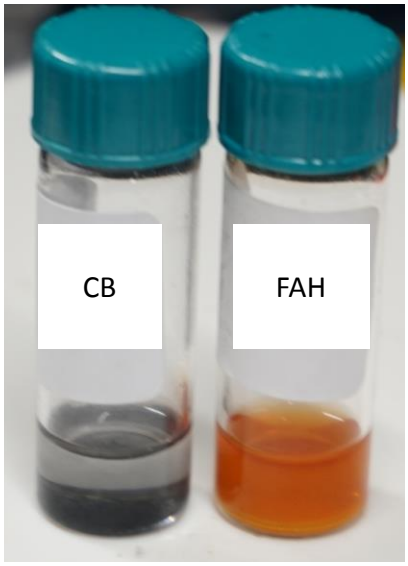

Figure S14: Optical image of $MAPbI_3$ powder in CB and FAH.

Isothermal Growth

To verify that this crystallisation effect is completely independent of temperature we crystallise the iodide, bromide and chloride systems isothermally at 70, 55, and 70 °C respectively. Details are the same as given in the Experimental Details section above with the following differences: (1) the solutions were dissolved at the crystallisation temperature and filtered through a 0.2 um syringe filter into two vials (1 control and 1 for acid addition), (2) the acid was preheated in the same oil bath for ~30 minutes before addition, and (3) vials were removed from the bath long enough to add the acid to the solution and agitate by hand until visible cloudiness was removed (typically 1-2 minutes). Results for the iodide and bromide system are shown in Fig. 1a in the main text.

Measurement of onset of crystallization

We prepared 1 M solution of the bromide salts in DMF. We then used a closed cap vial with the solution placed in an oil bath to monitor the onset of temperature of crystallization as a function of addition of formic acid (FAH). The temperature range was 20-100 °C and the step size was 10 °C .We waited 5 minutes at each temperature so see whether crystallization has

occurred or not by visual inspection. Once we saw crystallization, we noted the temperature and allowed the bath to come to 20 °C (ambient temperature) and the crystals to dissolve back in the solution. We then added few µls of FAH to vial and repeat the experiment to note the onset temperature. The experiment was repeated to see the effect of additional formic acid on the onset temperature of crystallization. Figure S15 shows the correlation between added FAH and onset temperature for crystallization.

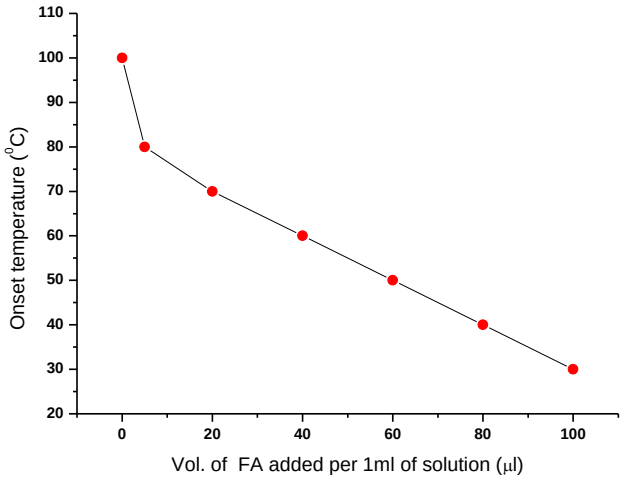

Figure S15: Onset temperature for crystallization of $CH_3NH_3Br_3$ versus the volume of FAH added in the salt solution

<u>$CsPbBr_3$ crystals:</u>

We prepared 0.33 M solution of $PbBr_2$ and CsBr in DMSO and added 20 vol % of formic acid. By heating the resulting solution at 120 °C for 10 minutes, we produced single crystals of $CsPbBr_3$. XRD single crystal diffraction and photoluminescence spectra confirmed the formation of $CsPbBr_3$ crystals.

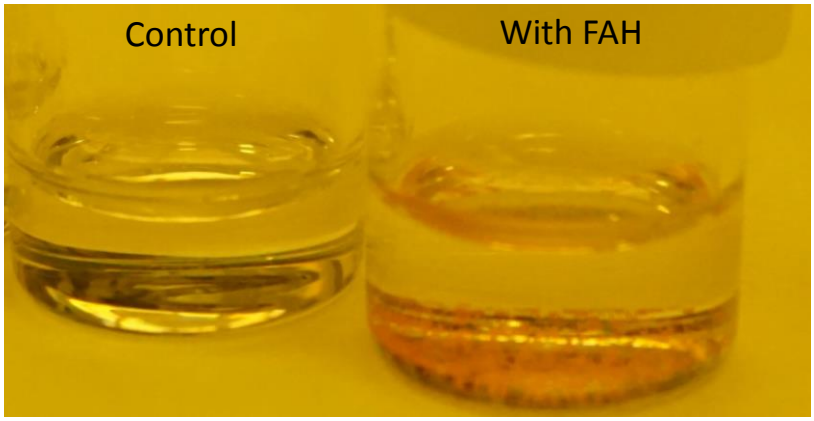

Figure S16: Growth of $CsPbBr_3$ in DMSO with FAH.

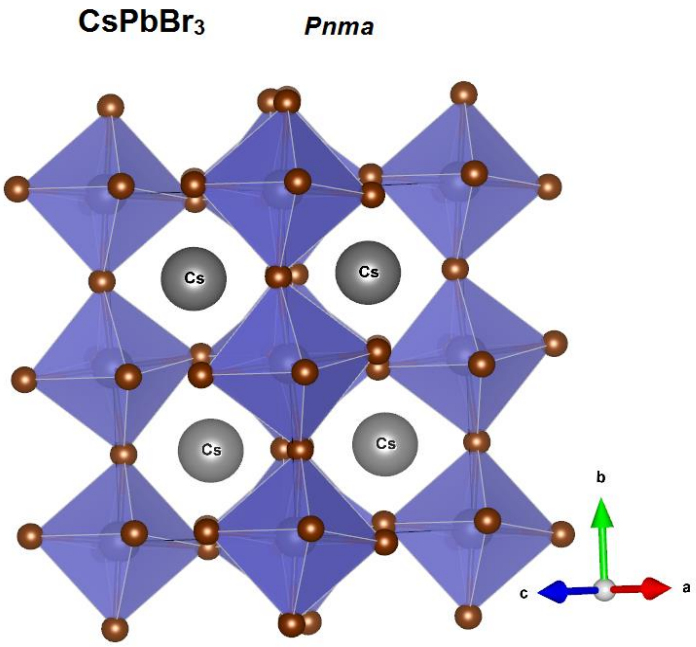

Figure S17 : Crystal structure of $CsPbBr_3$

Table S2: Crystallographic data for a $CsPbBr_3$ single crystal

Compound	$CsPbBr_3$
Measurement temperature	293 K
Crystal system	Orthorhombic
Space group	*P n m a* (no.62)
Unit cell dimensions	a = 8.250 ± 0.005 Å, b= 11.748 ± 0.005 Å, c = 8.205 ± 0.005

	Å, α = β = γ = 90°
Volume	2319.32 $Å^3$
Z	4
Density (calculated)	4.843 g/cm^3
Reflections collected	10130
Unique reflections	708 from which 0 suppressed
R(int)	0.0853
R (sigma)	0.0411
Goodness-of-fit	1.246
Final R indices (R_{all})	0.0347
wR_{obs}	0.0924
Wavelength	0.71073 Å
Weight scheme for the refinement	Weight = 1 / [$sigma^2(Fo^2)$ + (0.0315 * P)^2 + 0.00 * P] where P = (Max (Fo^2, 0) + 2 * Fc^2) / 3
Atomic Wyckoff-positions	Atom Site x y z site occupancy Cs 4a 0 0.5 0 1 Pb 4c -0.47055 0.25 0.00631 1 Br1 8d 0.29289 0.47563 0.20664 1 Br2 4c 0.00336 0. 75 0.04591 1
Isotropic temperature factors ($Å^2$)	U_{iso} (CS) 0.08637 ± 0.00065, (Pb) 0.03033 ± 0.00034 , (Br1) 0.07510 ± 0.00070, (Br2) 0.08594 ± 0.00103
Anisotropic temperature factor ($Å^2$)	$U_{11}(Cs)$ = 0.09940 ± 0.00144, $U_{11}(Pb)$ = 0.03053 ± 0.00051, $U_{11}(Br1)$ = 0.05998 ± 0.00113, $U_{11}(Br2)$ = 0.11628 ± 0.00274 U_{22}(Cs) = 0.06517± 0.00129, $U_{22}(Pb)$ = 0.02767 ± 0.00048, $U_{22}(Br1)$ = 0.10608 ± 0.00159, $U_{22}(Br2)$ = 0.02648 ± 0.00133 $U_{33}(Cs)$ = 0.09455 ± 0.00144, $U_{33}(Pb)$ = 0.03279 ± 0.00050, $U_{33}(Br1)$ = 0.05925 ± 0.00103, $U_{33}(Br2)$ = 0.11505 ± 0.00224

Extended Growth Parameters

Table S3: General survey of crystal/processing systems reported using rapid-crystallisation pathway studied here.

Salts	Solvent(s)	Previously Reported Temp. Range [°C]	Current Work Temp Range [°C]
MAI + PbI_2	GBL	90-190	48-150
MABr + $PbBr_2$	DMF	50-110	20-110
MABr + $PbBr_2$	NMP	n/a	80
MABr + $PbBr_2$	DMSO	n/a	105
MACl + $PbCl_2$	DMSO	100	50-80

Measurement of yield for crystallization:

We prepared 1 M solution of the bromide salts in 10 ml of DMF. We then used two closed cap vials each with half of the salt solution to grow the crystals. To one of the vials we added 100 µl of formic acid (FAH) and then placed both in an oil bath at 90 °C to grow crystals. After 30 minutes, we collected the $CH_3NH_3PbBr_3$ crystals, followed by a washing with dry diethyl ether and drying in an oven at 65 °C for 10 minutes. We then weighed the crystals to calculate the yield. We found that the yield of the crystals formation was 45% from the vial with FAH, compared to 35% from the control. We then brought the vials to room temperature and again added another 100µl of FAH to the vial already with FAH, then put both the vials again in the oil bath for another 30 minutes. We did not notice any growth of crystals in the control vial whereas the vial with FAH yielded more crystals which were collected as described before. We repeated the experiment with further addition of FAH followed by collection of crystals. We found that while the control vial did not yield more crystals after the initial incubation, incremental addition of FAH can give a cumulative yield up to 85%.

Crystallographic data of $CH_3NH_3PbI_3$ grown at different temperatures:

Table S4: Crystallographic Data of $CH_3NH_3PbI_3$ single crystals grown at different temperatures

Compound	α-$CH_3NH_3PbI_3$ **(1)**	α-$CH_3NH_3PbI_3$ **(2)**	α-$CH_3NH_3PbI_3$ **(3)**
Growth temperature	328 K	343 K	373 K
Measurement temperature	293 K	293 K	293 K
Space group	*I*4/*m c m*	*I*4/*m c m*	*I*4/*m c m*
Unit cell dimensions	a = 8.878 ± 0.005 Å c = 12.643 ± 0.005 Å α = β = γ = 90°	a = 8.880 ± 0.005 Å c = 12.632 ± 0.005 Å α = β = γ = 90°	a = 8.916 ± 0.005 Å c = 12.545 ± 0.005 Å α = β = γ = 90°
Volume	996.73 $Å^3$	996.08 $Å^3$	997.26 $Å^3$
Z	4	4	4
Density (calculated)	4.131 g/cm^3	4.134 g/cm^3	4.132 g/cm^3
Reflections collected	7946	5937	6131
Unique reflections	261	257	260
Inconsistent equivalents	10	18	8
R(int)	0.1255	0.1212	0.0881
R (sigma)	0.0278	0.0265	0.0245
Goodness-of-fit	1.217	2.094	1.419
Final R indices	0.0560	0.0771	0.1269
Twin model	[0 1 0 1 0 0 0 -1]	More than one twin	More than one twin
Extinction coefficient	0.028696	0.005836	0.008768
Wavelength	0.71073 Å	0.71073 Å	0.71073 Å

Weight scheme for the refinement	Weight = 1 / [sigma^2 (Fo^2) + (0.0681 * P)^2 + 82.13 * P] where P = (Max (Fo^2, 0) + 2 * Fc^2) / 3	Weight = 1 / [sigma^2 (Fo^2) + (0.0681 * P)^2 + 82.13 * P] where P = (Max (Fo^2, 0) + 2 * Fc^2) / 3	Weight = 1 / [sigma^2(Fo^2) + (0.0529 * P)^2 + 642.71 * P] where P = (Max (Fo^2, 0) + 2 * Fc^2) / 3

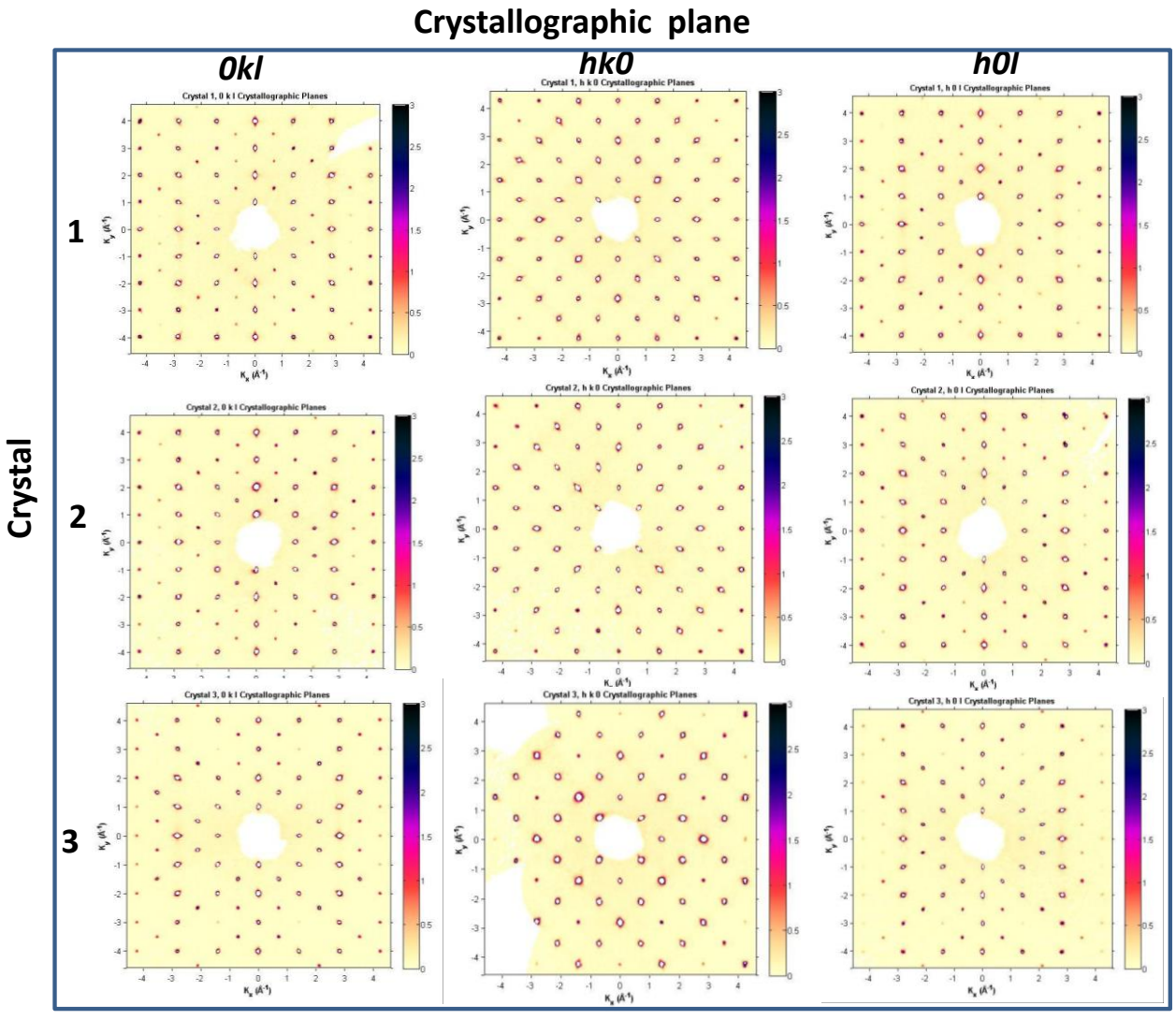

Figure S18 : Unwarped precession images of $CH_3NH_3PbI_3$ crystals (see table S2) in different crystallographic planes 0kl , hk0 and h0l.

The diffraction patterns from the crystals grown at 55 °C are fit with only a single twin, and they exhibit the best fit against the calculated diffraction pattern. Another key observation is that the crystal structure we refine from the crystals grown at differing temperatures have significant differences. For a cubic perovskite lattice, we expect there to be no rotational tilt between the adjacent lead halide octahedra, for a tetragonal lattice we expect this tilt to exist. Interestingly, the tilt angle between adjacent octahedra is larger for the crystals grown at 55 °C than those grown at 100 °C, exemplifying the importance of controlling the temperature of the crystallisation in order to control the crystal structure, and hence the resulting electronic properties.

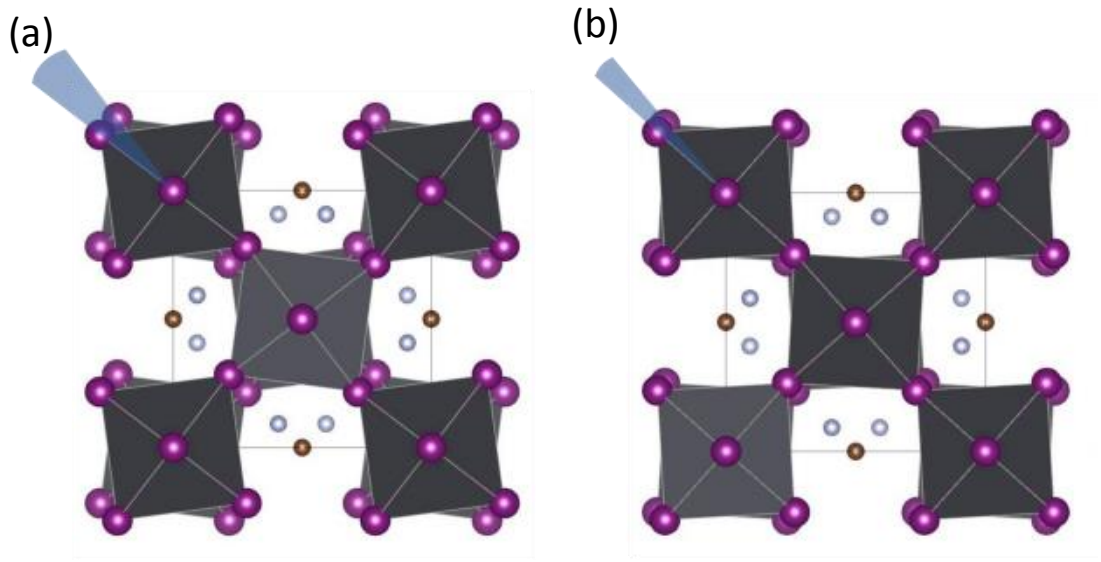

Figure S19: Refined crystal structure of $MAPbI_3$ single crystals viewed along the c-axis grown at a) 55 ˚C and b) 100 ˚C. The octahedral tilting (Glazer tilt i.e. a°a°c⁻) is illustrated by the dihedral angle (blue area).

1P and 2P Photoluminescence:

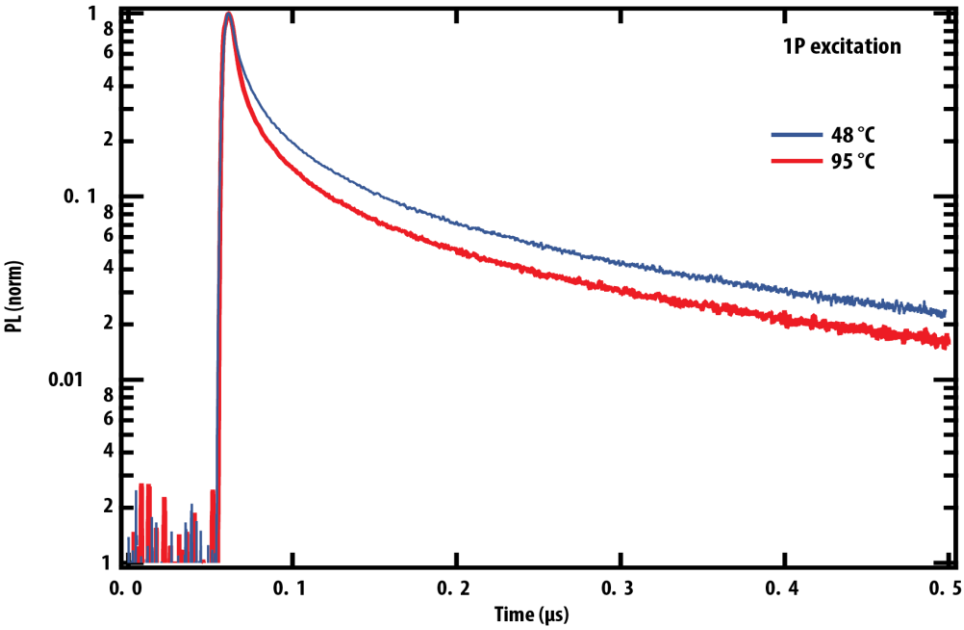

Figure S20: Photoluminescent transient of $CH_3NH_3PbI_3$ single crystals grown at 48˚C (below the tetragonal to cubic phase transition) and at 95˚C. under 1P excitation (λ_{ex} = 532 nm).

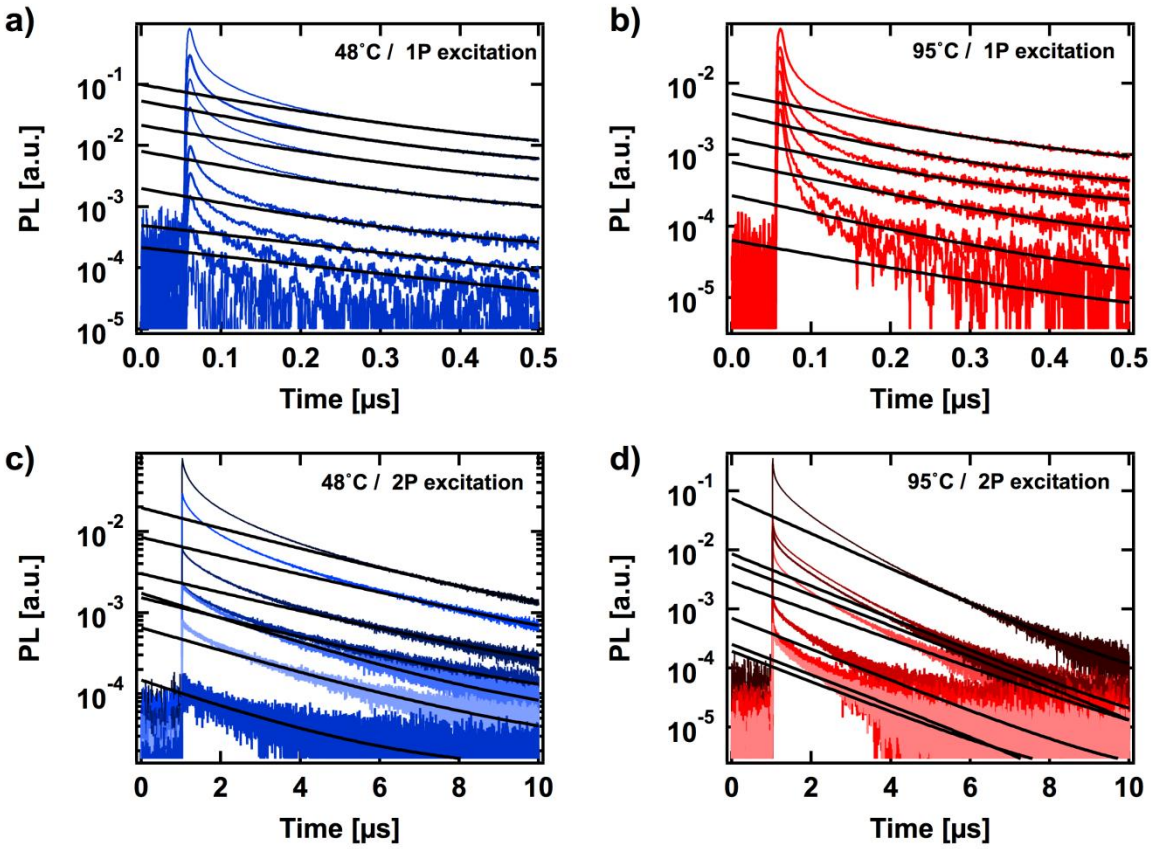

Figure S21: Decay traces from single crystals grown at 48˚C and 95˚C under 1 photon excitation (a, b) and 2 photon excitation (c, d). The slow part of the decays is fitted with a single exponential to estimate the SRH recombination constant k_1.

References:

1. Hidalgo, R., Ash, P.A., Healy, A.J., Vincent, K.A. Infrared Spectroscopy During Electrocatalytic Turnover Reveals the Ni-L Active Site State During H_2 Oxidation by a NiFe Hydrogenase. *Angew. Chemie. Int. Ed.* **127**, 7216-7219 (2015).
2. Ortega-Arroyo, J.; Kukura, P., Interferometric Scattering Microscopy (Iscat): New Frontiers in Ultrafast and Ultrasensitive Optical Microscopy. *Physical chemistry chemical physics : PCCP* **2012**, *14*, 15625-36.
3. Ortega Arroyo, J.; Cole, D.; Kukura, P., Interferometric Scattering Microscopy and Its Combination with Single-Molecule Fluorescence Imaging. *Nat. Protocols* **2016**, *11*, 617-633.
4. Zeroka, D. & Jensen, J. O. Infrared spectra of some isotopomers of methylamine and the methylammonium ion: a theoretical study. *J. Mol. Struct. THEOCHEM* **425,** 181–192 (1998).
5. Max, J.-J. & Chapados, C. Infrared Spectroscopy of Aqueous Carboxylic Acids: Comparison between Different Acids and Their Salts. *J. Phys. Chem. A* **108,** 3324–3337 (2004).
6. Cox, B. G. *Acids and Bases*. **16,** (Oxford University Press, 2013).
7. Trusell, F. Determination of the extent of acid hydrolysis of N-methylpyrrolidone. *Talanta* **13**, 1043-1045 (1966).